

**PSFC/JA-07-7**

**Electron collection by a negatively charged sphere in a  
collisionless magnetoplasma**

L. Patacchini  
I. H. Hutchinson  
G. Lapenta\*

\* Centrum voor Plasma-Astrofysica, Departement Wiskunde, Katholieke Universiteit  
Leuven, Celestijnenlaan 200B, 3001 Leuven, Belgium.

**Plasma Science and Fusion Center  
Massachusetts Institute of Technology  
Cambridge MA 02139 USA**

Submitted for publication to *Physics of Plasmas*.

This work was supported by the U.S. Department of Energy, Grant No. DE-FG02-06ER54891. Reproduction, translation, publication, use and disposal, in whole or in part, by or for the United States government is permitted.

## Abstract

Easy-to-evaluate approximate formulas are presented for the repelled-species current collected by a spherical body in a collisionless, magnetized plasma, valid over the full range of ratio of Larmor radius to sphere radius. The form is an appropriate average of the lower and upper bounds obtained by prior analytic arguments. This formulation enables rapid evaluation of the floating potential in hybrid Boltzmann - Particle In Cell (PIC) codes with a background magnetic field. The treatment is validated by comparison of hybrid PIC (ion particle) code with full PIC (electron and ion particle) code calculations. It is found that typically for no value of magnetic field is it valid to approximate the electrons as fully magnetized but the ions as unmagnetized in the absence of plasma drift.

## 1 Introduction

The calculation of the current drawn by a spherical electrode from a collisionless plasma is important to understand the charging of dust particles or the characteristics of Langmuir probes ; but it is a non-linear problem of considerable complexity and computational cost. It can often be simplified by the assumption that the repelled species (usually electrons) adopt a Boltzmann distribution [1] :

$$n_e(\mathbf{r}) = n_\infty \exp\left(\frac{eV(\mathbf{r})}{T_e}\right), \quad (1)$$

where  $V(\mathbf{r})$  is the electrostatic potential,  $n_e(\mathbf{r})$  and  $T_e$  the electron density and temperature, and  $n_\infty$  the electron density at infinity. We denote by  $v_{te} = \sqrt{\frac{2T_e}{m_e}}$  the electron thermal velocity.

Using Liouville's theorem, the repelled-species flux density to a stationary collector surface of convex shape with potential distribution  $V_p(\sigma)$  (where  $\sigma$  denotes surface position) is determined by the constancy of the distribution function along particle orbits, and is equal to the free-space one-dimensional flux density scaled down by the same factor as  $n_e$ :

$$\Gamma_e^{convex}(\sigma) = n_\infty \exp\left(\frac{eV_p(\sigma)}{T_e}\right) \frac{v_{te}}{2\sqrt{\pi}} \quad (2)$$

provided that all incoming orbits at the probe actually connect back to the distant plasma. (This is the meaning of "convex"). The total current to a spherical probe, possibly insulating, is then given by integrating Eq. (2) over its surface :

$$I_e = \int_{Sphere} \Gamma_e^{convex}(\sigma) d\sigma. \quad (3)$$

The approximation that the distant electron distribution is effectively an (unshifted) Maxwellian, which is required for this Boltzmann treatment, Eq. (1), is justified even for flowing plasmas if  $v_{te}$  is much larger than typical flow velocities. Therefore it is useful for hybrid particle codes.

The derivation of Eq. (2) however assumes that all the orbits striking the probe are connected to infinity. When a background magnetic field is present this is no longer a good approximation. The flux is reduced because some helicoidal orbits intersect the probe several times. Orbit arcs that intersect the sphere at both ends are unpopulated. See Fig. (1).

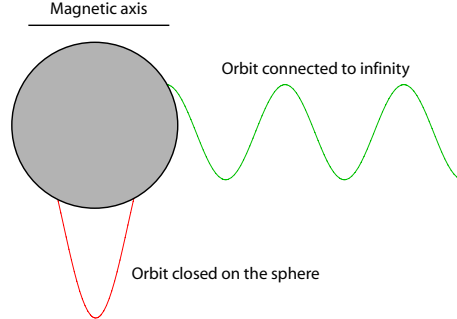


Figure 1: Schematic representation of the two kind of orbits intersecting the probe in the presence of a background magnetic field. In a collisionless plasma orbits that close on the sphere are empty. The magnetic field polarity is irrelevant for our purposes.

When the Larmor radius is much larger than the sphere radius  $r_p$ , that is in the limit  $B = 0$ , then no such empty orbits exist and one can use Eq. (2), giving for the total current to an equipotential repelling sphere of radius  $r_p$  :

$$I_e^{B=0} = 4\pi r_p^2 n_\infty \frac{v_{te}}{2\sqrt{\pi}} \exp\left(\frac{eV_p}{T_e}\right). \quad (4)$$

In the opposite limit of infinitesimal Larmor radius, the electrons move one-dimensionally along the field, and encounter only the projection of the probe area ( $2\pi r_p^2$ , where the 2 is due to the electrons coming from both sides of the probe) in the field direction. Therefore the current instead becomes, for  $B = \infty$  :

$$I_e^{B=\infty} = 2\pi r_p^2 n_\infty \frac{v_{te}}{2\sqrt{\pi}} \exp\left(\frac{eV_p}{T_e}\right), \quad (5)$$

half as large.

The problem of correcting Eq. (3) in the intermediate case with finite electron Larmor radius, was tackled by Rubinstein and Laframboise [2], who found and evaluated expressions for lower and upper bounds (more restrictive than Eqs (4,5)) to the total electron current  $I_e$  collected by a conducting probe. Sonmor and Laframboise [3] calculated numerically the repelled species current in the case of negligible space-charge, that is, when the shielding length  $\lambda_s$  is much larger than the probe radius. The shielding length can be considered to be the factor occurring in the linearized approximation to the potential profile (the Debye-Hückel formula)  $V \propto \exp(-(r - r_p)/\lambda_s)/r$  ; often this is approximated as  $\lambda_s^{-2} = \lambda_{De}^{-2} + \lambda_{Di}^{-2}$ , where  $\lambda_{De}$  and  $\lambda_{Di}$  are the electron and ion Debye lengths. Here and in the rest of the paper, quantities labeled by the index “i” refer to the ion species.

The electron density even in most magnetized cases can still be described by Eq. (1). The error in this expression is small, regardless of gyro orbit effects, in regions where most of the electrons have insufficient total energy to overcome the repulsive probe potential. The overall effect of the approximation on the potential profile will be ignorable provided the probe potential is substantially more negative than  $-T_e/e$ .

The purpose of this work is to develop an empirical expression that is easy to evaluate for the electron collection flux, valid for a wide range of shielding lengths and magnetic fields. This expression is implemented in the hybrid Particle In Cell (PIC) code SCEPTIC [4]. That enables it to determine the floating potential when the plasma is magnetized. This upgrade of SCEPTIC is benchmarked against full PIC simulations using the code *Democritus* [5].

As a concrete application of the new possibilities of SCEPTIC we compute the floating potential of a stationary probe in the presence of a weak magnetic field, and compare it with a modified Orbital Motion Limited (OML) theory where only the electrons are assumed to be magnetized.

## 2 Current to a conducting, repelling spherical probe

### 2.1 Laframboise and Rubinstein's Upper and Lower bounds

The electron current when  $0 < B < \infty$  lies between the values given by Eq. (4) and Eq. (5). Rubinstein and Laframboise have shown that it is possible to improve the lower bound given by Eq. (5) [2]. The idea is to assume that the effects of orbit depletion due to multiple intersections with the probe occur in a neighborhood of the probe where the electrons have already been decelerated by  $eV_p$ . The distribution function at the entrance of this neighborhood is then purely Maxwellian, and then one needs to find the fraction of purely helical orbits (unaffected by local electric field) that when traced backwards from the probe extend to infinity without intersecting the probe again.

Hereafter, the potentials named  $\phi$  are scaled to  $\frac{T_e}{e}$ . For the electrons, the Liouville theorem tells us that the distribution function of particles having a  $\mathbf{z}$ -velocity directed towards the probe at the neighborhood entrance is :

$$f(\mathbf{v}) = n_\infty \exp(\phi_p) \frac{1}{(v_{te}\sqrt{\pi})^3} \exp\left(-\frac{\mathbf{v}^2}{v_{te}^2}\right) \quad (6)$$

We now need to calculate the electron current collected by a sphere at space potential (i.e.  $\phi_p = 0$ ) in a Maxwellian plasma but accounting for the helical orbits. This was performed the first time by Whipple [6], and can be recovered by setting  $D = 0$  and  $\chi_p = 0$  in Eq. (9) from [2]. The result is expressed in terms of the non-dimensional quantity  $\iota$  equal to the current divided by  $4\pi r_p^2 n_\infty v_{te}/2\sqrt{\pi}$ , plotted in Fig. (2). It only depends on the non-dimensional factor  $\beta_e$ , which is a measure of the magnetic field defined as the ratio of the probe radius over a mean electron gyroradius  $r_L$ .

$$\beta_e = \frac{r_p}{\sqrt{\frac{\pi T_e m_e}{2e^2 B^2}}} \quad (7)$$

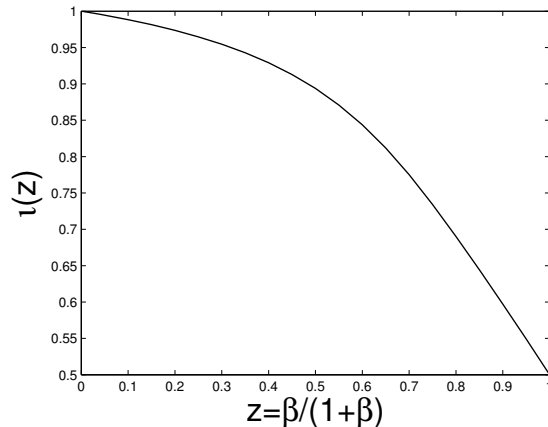


Figure 2: Electron (Ion) current collection by a spherical probe at space potential (normalized to  $4\pi r_p^2 n_\infty \frac{v_{te}(t_i)}{2\sqrt{\pi}}$ ) as a function of the magnetic field  $\beta_e$  ( $\beta_i$ ). If  $\beta = 0$ , the particle current is simply the sphere area times the random flux density :  $\iota(0) = 1$ . If  $\beta = \infty$ , the particle current is reduced by a factor of 2 :  $\iota(1) = 1/2$ .

The factor  $\iota$ , illustrated in Fig. (2), can be approximated to within 0.3% by :

$$\iota^*(z) = 1.000 - 0.0946z - 0.305z^2 + 0.950z^3 - 2.200z^4 + 1.150z^5 \quad \text{with} \quad z = \frac{\beta_e}{1 + \beta_e}. \quad (8)$$

Eq. (8) has been obtained by polynomial fitting over the range  $z \in [0 : 1]$ , and is therefore different from the Taylor expansion of  $\iota$  at  $z = 0$ . Here and in the rest of the paper,  $Q^*$  denotes the empirical formula corresponding to the physical quantity  $Q$ . In this precise case  $Q$  is  $\iota$ .

In the helicoidal orbit approximation we have for the electrons :

$$I_e^{Low} = 4\pi r_p^2 \frac{v_{te}}{2\sqrt{\pi}} \iota(z) \exp(\phi_p) \quad (9)$$

This expression will be equal to the “true” electron current  $I_e$  when the potential is actually constant in the neighborhood of the probe. The effect of a repelling potential gradient upon an orbit that we trace backwards from its intersection with the probe is to decrease its probability of reintersecting with the probe. Since the reduction in current (the extent to which  $\iota$  is less than 1) is attributable purely to the depopulation of orbits that intersect the probe more than once, reducing the fraction of such orbits increases the current to the probe. In other words, the expression (9) is a lower bound for the collected current of repelled species, while the expression (4) is an upper bound.

We recall here for completeness that an improvement of the upper bound given by Eq. (4) can be made using conservation of canonical angular momentum about the  $\mathbf{B}$ -axis. Rubinstein and Laframboise calculate the region where a particle’s presence is permitted by energy and canonical angular momentum conservation, called the “magnetic bottle”. An

upper bound on the collected current is obtained by assuming that a particle will strike the collector if its magnetic bottle will. The result, given in analytic form in Eqs (36,37) of [2], will not be used in this paper.

## 2.2 Empirical expression of $I_e$ when $\lambda_s = \infty$

How close to each of the bounds the real current will be depends, *a priori*, on  $\phi_p$ , the potential distribution (through  $\lambda_s$ ), and  $\beta_e$ . If we assume that  $\lambda_s \gg r_p$ , the potential is Coulomb around the probe and  $\lambda_s$  is removed from the parameters.

Under this assumption, the electron current can easily be computed by direct orbit integration. We used SCEPTIC with a prespecified Coulomb potential, and calculated  $I_e$  for a wide range of  $\beta_e$  and  $\phi_p$ . The results are plotted in Fig. (3), and their validity assessed by comparison with a similar computation performed by Sonmor and Laframboise [3].

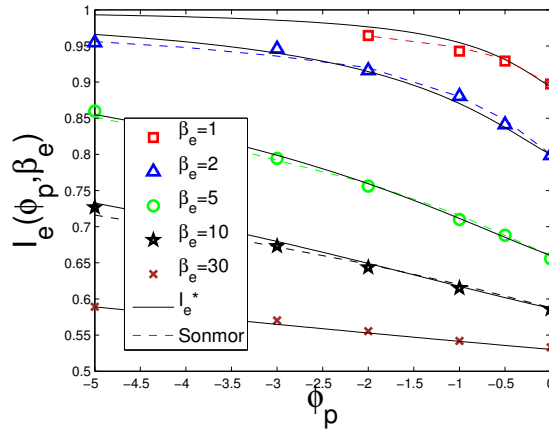


Figure 3: Electron current collection (normalized to  $4\pi r_p^2 \frac{v_{te}}{2\sqrt{\pi}} \exp(\phi_p)$ ) as a function of the probe potential ( $\phi_p$ ) for different magnetic fields under the assumption of large  $\lambda_s$  calculated by direct orbit integration with SCEPTIC. The dashed lines represent the Sonmor and Laframboise results for the same computation (See Fig. (13) from [3]). Also plotted in solid lines are the empirical values  $I_e^*$  given by Eq. (13).

To first order in  $r_p$  the potential variation around the probe is linear and has a slope  $\frac{d\phi}{dr} \Big|_{r=r_p} = -\frac{\phi_p}{r_p}$ . What is more, in the limit  $\beta_e \gg 1$  the electrons see the probe as flat in their last Larmor gyrations. The two parameters governing the demagnetization of the electrons, and therefore the departure of  $I_e$  from  $I_e^{Low}$ , are  $\frac{\phi_p}{r_p}$  and  $r_L$ . Elementary dimensional analysis shows that the only relevant parameter for this problem is :

$$\eta = -\frac{\phi_p}{\beta_e} \quad (10)$$

This argument is no longer valid when  $\beta_e \lesssim 1$ , in which case demagnetization of the electrons is expected to depend on  $\phi_p$  and  $\beta_e$  separately. However for such low magnetic fields  $I_e^{Low}$  is close to  $I_e^{Up} = I_e^{B=0}$  (See Fig. (3)), and still using  $\eta$  as unique parameter proves satisfactory.

We express  $I_e$  in the form :

$$I_e = A(w)I_{Up} + (1 - A(w))I_{Low} \quad \text{with} \quad w = \frac{\eta}{1 + \eta} \quad (11)$$

Here  $A$  is the demagnetization function, plotted in Fig. (4) using the data from Fig. (3). For small  $\eta$ ,  $A$  is indeed only a function of  $\eta$ . For large  $\eta$  this is not the case anymore, and we chose  $A^*$  in order to fit the points corresponding to  $\beta_e = 2$ .

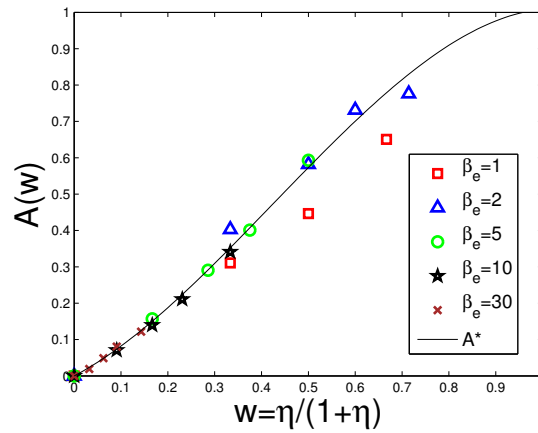


Figure 4: Plot of the demagnetization function  $A$  as a function of  $\eta$ . The values of  $A$  computed by direct orbit integration (points) only depend on  $\eta$ , except for large  $\eta$  where  $A$  is a separate function of  $\phi_p$  and  $\beta_e$ .

A third order polynomial fit to the demagnetization function is :

$$A^*(w) = 0.678w + 1.543w^2 - 1.212w^3 \quad (12)$$

In summary, an empirical formula for the electron current is given by :

$$I_e^* = 4\pi r_p^2 [A^*(w) + (1 - A^*(w))t^*(z)] \frac{v_{te}}{2\sqrt{\pi}} \exp(\phi_p) \quad (13)$$

### 2.3 Extension to $\lambda_s \neq \infty$

Fig. (5) shows the effect of a finite  $\lambda_s$  on the electron collection. For this qualitative purpose, a Debye-Hückel potential distribution has been assumed.

$$\phi(r) = \phi_p \frac{r_p}{r} \exp\left(-\frac{r - r_p}{\lambda_s}\right) \quad (14)$$

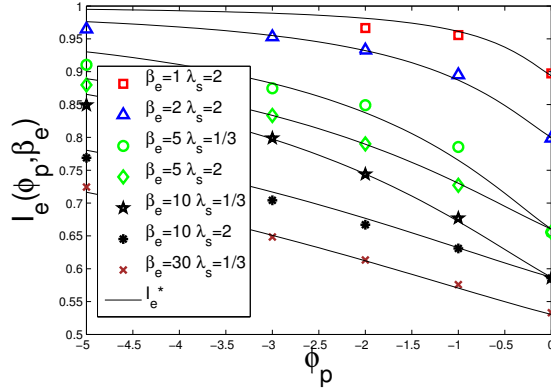


Figure 5: Electron current collection (normalized to  $4\pi r_p^2 \frac{v_{te}}{2\sqrt{\pi}} \exp(\phi_p)$ ) as a function of the probe potential for different  $\lambda_s$  and  $\beta_e$ , obtained by direct orbit integration in a Debye-Hückel potential. Also shown in solid lines are the empirical values  $I_e^*$ .

The screening shortening increases the electron current, because the potential derivative at the probe edge rises. For the potential distribution given by Eq. (14),  $\frac{d\phi}{dr} \Big|_{r=r_p} = -\frac{\phi_p}{r_p} \left(1 + \frac{r_p}{\lambda_s}\right)$ . A first correction to  $I_e^*$  (Eq. (13)) is readily obtained by setting  $\eta = -\frac{\phi}{\beta_e} \left(1 + \frac{r_p}{\lambda_s}\right)$ .

This form however does not prove satisfactory if  $r_L > \lambda_s$ . The physical reason being that in this situation the electrons do not see a linearly varying potential in their last Larmor gyration. A heuristic correction yielding the good limit at low  $\frac{r_L}{\lambda_s}$  is :  $1 + \frac{\beta_e}{\alpha} \left(1 - \exp\left(\frac{-\alpha r_p}{\lambda_s \beta_e}\right)\right)$ . We chose  $\alpha = 4$  in order to maximize the agreement with the data of Fig. (5).

The electron current  $I_e^*$  in a plasma of finite  $\lambda_s$  is therefore approximated by Eqs. (12, 13) with :

$$\eta = -\frac{\phi}{\beta_e} \left(1 + \frac{\beta_e}{4} \left(1 - \exp\left(\frac{-4r_p}{\lambda_s \beta_e}\right)\right)\right) \quad (15)$$

### 3 Current to an insulating, repelling spherical probe

#### 3.1 Expression of the electron flux

We have so far focused on the total collected current  $I_e$ . If the probe is insulating, or if the current density to different positions on the probe is measured, important information lies in the electron flux  $\Gamma_e$  as a function of the position on the sphere surface, parameterized as shown in Fig. (6).

The function  $\Gamma_e(\sigma)$ , where  $\sigma = (\cos\theta, \varphi)$  depends on  $\beta_e$ ,  $\lambda_s$ , and *a priori* on the whole potential distribution  $\phi_p(\sigma)$ .

Fig. (7) shows  $\Gamma_e(\cos\theta)$  for a conducting probe at different values of  $\beta_e$ . In this case the problem is independent of  $\varphi$ . We see that  $\Gamma_e(|\cos\theta| = 1) = \frac{v_{te}}{2\sqrt{\pi}} \exp(\phi_p)$  regardless of the



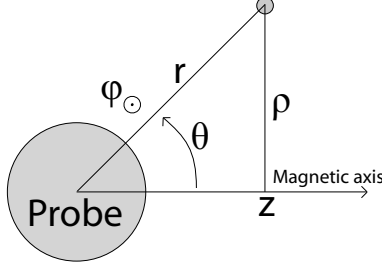


Figure 6: Schematic of the coordinate system.  $\mathbf{B}$  is parallel to  $\mathbf{z}$ .

magnetic field. Since we also know that in the limit of a strong magnetic field  $\Gamma_e(\cos \theta) = \frac{v_{te}}{2\sqrt{\pi}} \exp(\phi_p) |\cos \theta|$ , a natural approximate form to adopt for  $\Gamma_e^*$  is a downward pointing triangle with value at  $|\cos \theta| = 1$  independent of  $\beta_e$ , and  $2\pi r_p^2 \int_{-1}^1 \Gamma_e^*(\cos \theta) d \cos \theta = I_e^*$ , that is :

$$\Gamma_e^*(\cos \theta) = \left[ \frac{2I_e^*}{4\pi r_p^2} - \frac{v_{te}}{2\sqrt{\pi}} \exp(\phi_p) \right] + 2 \left[ \frac{v_{te}}{2\sqrt{\pi}} \exp(\phi_p) - \frac{I_e^*}{4\pi r_p^2} \right] |\cos \theta| \quad (16)$$

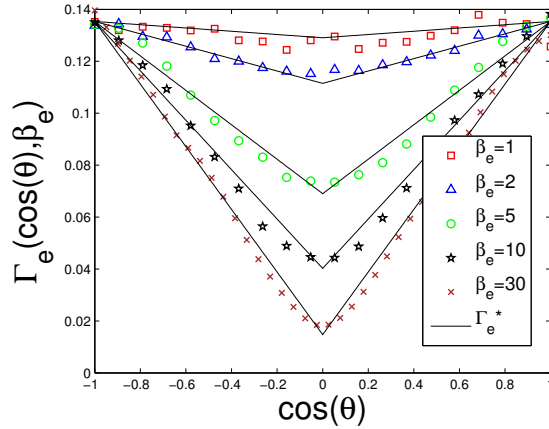


Figure 7: Electron flux (in units of  $v_{te}/2\sqrt{\pi}$ ) to a conducting sphere of bias  $\phi_p = -2$  with  $\lambda_s = \infty$  at different magnetic field strengths computed by direct orbit integration, as well as  $\Gamma_e^*$  (Eq. (16)).

The preceding analysis is only valid for an equipotential sphere. However if  $\beta_e$  is large enough, the electrons will see a uniform potential at the probe surface during their last Larmor gyration before collection. In other words  $\Gamma_e(\sigma)$  will depend on the local potential,  $\phi_p(\sigma)$ , but not on the value of  $\phi_p$  at other angles. One can therefore use the following extension to Eq. (16).

$$\Gamma_e^*(\sigma) = \left[ \frac{2I_e^*(\sigma)}{4\pi r_p^2} - \frac{v_{te}}{2\sqrt{\pi}} \exp(\phi_p(\sigma)) \right] + 2 \left[ \frac{v_{te}}{2\sqrt{\pi}} \exp(\phi_p(\sigma)) - \frac{I_e^*(\sigma)}{4\pi r_p^2} \right] |\cos \theta|. \quad (17)$$

$I_e^*(\sigma)$  (Eq. (13)) is the total electron current that would be collected by a conducting probe at bias  $\phi_p(\sigma)$  with a shielding length  $\lambda_s(\sigma)$ .

Eq. (17) is valid for an insulating sphere with arbitrary two-dimensional potential distribution, provided the convention  $\mathbf{B} \parallel \mathbf{z}$  is adopted. Eq. (17) does not involve the magnetic field polarity. In other words the electron flux density distribution to a probe with arbitrary potential distribution, be it non symmetric about the magnetic axis, will be unchanged by the operation  $\mathbf{B} \rightarrow -\mathbf{B}$ .

### 3.2 Validity of $\Gamma_e^*$ for a concrete example

In the case of a plasma drifting parallel to  $\mathbf{B}$  and  $\mathbf{z}$ , the ion flux and hence the probe potential are higher upstream than downstream. A crude approximation to this situation would be to model the probe potential by the first two terms of a spherical harmonic expansion :

$$\phi_p(\cos \theta) = -2\left(1 + \frac{1}{3} \cos \theta\right). \quad (18)$$

We recall that  $\phi$  is normalized to  $\frac{T_e}{e}$ . The coefficients of Eq. (18) are arbitrary, and only serve the purpose of verifying Eq. (17).

Fig. (8) shows the electron flux collected by a probe in a plasma with uniform  $\lambda_s = 2$  and potential distribution given by :

$$\phi(r, \cos \theta) = \phi_p(\cos \theta) \frac{r_p}{r} \exp\left(-\frac{r - r_p}{\lambda_s}\right). \quad (19)$$

We see that even for rather small magnetic fields, it is a good approximation to assume that  $\Gamma_e(\sigma)$  only depends on  $\phi_p(\sigma)$ . The difference between the total current calculated using Eq. (17) and the corresponding ‘‘exact value’’ is systematically limited to 2%. Similar test cases with a potential distribution depending on both  $\cos \theta$  and  $\varphi$  have been performed as well, and lead to the same conclusions.

## 4 Application to hybrid PIC codes

### 4.1 SCEPTIC upgrade

SCEPTIC [4] is a 2d/3v hybrid Boltzmann-PIC code written in spherical coordinates centered on a spherical probe. The code is two dimensional in space, allowing the simulation of an axially symmetric flow (The drift velocity and the magnetic field must be parallel).

The code can be run in the floating potential regime by imposing a probe potential such as to equate the ion current with the electron current given by Eq. (4). For an unmagnetized case this is unproblematic. By using  $\Gamma_e^*$  (Eq. (17)) for the electron flux, we can now include

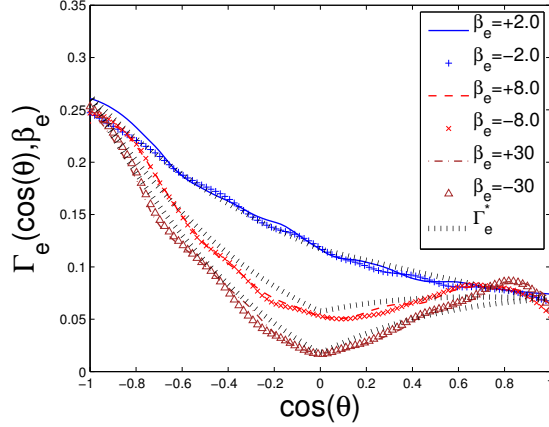


Figure 8: Electron flux to a sphere with non symmetric potential distribution given by Eqs. (18,19) for different magnetic fields computed by direct orbit integration, as well as  $\Gamma_e^*$  (Eq. (17)). It can be seen that the magnetic field polarity is indeed irrelevant.

a background magnetic field. The electron flux to each angular cell of the probe is computed with a self-consistently calculated  $\lambda_s$  :

$$\lambda_s(\theta) = -\frac{r_p}{\frac{r_p}{\phi(\theta)} \frac{d\phi(\theta)}{dr} + 1}. \quad (20)$$

If one wishes to use  $\Gamma_e^*$  for an analytical treatment and has not access to a self-consistent calculation for  $\lambda_s$ , the question arises of what value to choose for the shielding length. If  $\lambda_{De}$  is the electron Debye length, the linearized theory gives :

$$\lambda_L^2 = \lambda_{De}^2 \frac{1}{1 + ZT_e/(T_i + m_i v_d^2)}. \quad (21)$$

The term  $m_i v_d^2$  (twice the ion drift energy) has been suggested by Hutchinson [8] in order for  $\lambda_L$  to tend to  $\lambda_{De}$  if  $v_d \gg v_{ti}$ . As has been pointed out by Daugherty and al. [7] however, the shielding length can by far exceed  $\lambda_L$  when  $\lambda_{De}$  is smaller than a few  $r_p$ . A slight improvement can be made by choosing  $\sqrt{r_p^2 + \lambda_L^2}$  as the shielding length [8], but this form gives a shielding greater than  $r_p$ , which is obviously wrong if  $\lambda_{De} \ll r_p$ .

We therefore tabulated  $\lambda_s$  as given by Eq. (20) for a wide range of parameters ( $\lambda_{De} \in [0.05 : 3]r_p$ ,  $T_i \in [0.01 : 1]ZT_e$ ,  $v_d \in [0 : 1]\sqrt{ZT_e/m_i}$ ,  $\beta_i \in [0 : 0.2]$ ). The following expression for  $\lambda_s$ , yielding the correct limit for  $\lambda_{De} \gg r_p$ , has a better accuracy than the linearized form at low  $\lambda_{De}$  as can be seen on Fig. (9).

$$\lambda_s^* = \lambda_L + \lambda_{De} \ln\left(1 + \frac{r_p}{\lambda_{De}}\right). \quad (22)$$

Expression (22) has been crafted for weakly magnetized ions. It is independent of B because if  $\beta_i$  is small the ions follow unmagnetized orbits, and the electron density is Boltzmann

regardless of  $\beta_e$ . We recall here the relation  $\beta_e = \sqrt{m_i T_i / Z^2 m_e T_e} \beta_i$ . If the ions become too much magnetized we expect Eq. (22) to loose accuracy, but under those circumstances and for reasonable floating potentials  $I_e^*$  tends to  $I_e^{Low}$ , therefore using a slightly wrong shielding length is not problematic.

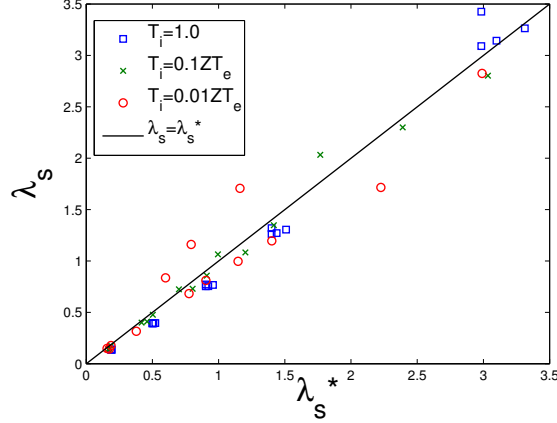


Figure 9:  $\lambda_s$  (Eq. (20)) against  $\lambda_s^*$  (Eq. (22)) for  $\lambda_{De} \in [0.05 : 3]r_p$ ,  $T_i \in [0.01 : 1]ZT_e$ ,  $v_d \in [0 : 1]\sqrt{ZT_e/m_i}$ ,  $\beta_i \in [0 : 0.2]$ . The points at  $\lambda_s^* \simeq 0.2r_p$  correspond to  $\lambda_{De} = 0.05r_p$ . Using  $\lambda_L$  for the shielding length would therefore be extremely inaccurate.

The expression (22) readily gives the sphere capacitance under a form independent of the magnetic field for  $\beta_i \leq 0.2$  :

$$C^* = 4\pi\epsilon_0 r_p \left(1 + \frac{r_p}{\lambda_s^*}\right) \quad (23)$$

## 4.2 Validation with the full PIC-code *Democritus*

*Democritus* [5] is a full PIC code (both the ions and electrons are self-consistently advanced) written in cylindrical coordinates allowing to simulate axially symmetric flows as in SCEPTIC. The probe is modeled by infinitely heavy particles with the immersed boundary technique, and the mesh is adaptative in order to accurately resolve the probe-plasma boundary.

As soon as the ions become magnetized, collisions and cross-field transport become essential for the magnetic presheath to merge with the plasma at infinity [1]. Therefore a full physical simulation of current collection by a collector in a magnetoplasma must be collisional and requires a computational domain extended a few ion mean free paths ( $\lambda_{mfp}$ ) along the magnetic axis (and at least two mean Larmor radii in the perpendicular direction). However since we are only interested in a code comparison we will relax this requirement, and use for SCEPTIC a spherical domain of radius  $r_b = 5r_p$ , and for *Democritus* a cylindrical domain of radius  $\rho = 5r_p$  and length  $z = 10r_p$ . We defer a complete collisional treatment to

a future publication, therefore in the absence of information on the collisional dynamics in the presheath we set the potential to  $\phi(r_b) = 0$  at the outer boundary.

We performed the validation on a conducting sphere with two different sets of parameters assuming  $m_i/(Zm_e) = 100$ ,  $T_i = ZT_e$ , and  $\lambda_{De} = 2r_p$ . For the first set (S1) :  $v_d = 0$  and  $\Omega_e = 15\omega_{pe}$  (i.e.  $\beta_e = 5.98$ ). For the second set (S2) :  $v_d = 0.5\sqrt{ZT_e/m_i}$  and  $\Omega_e = 30\omega_{pe}$  (i.e.  $\beta_e = 11.97$ ).

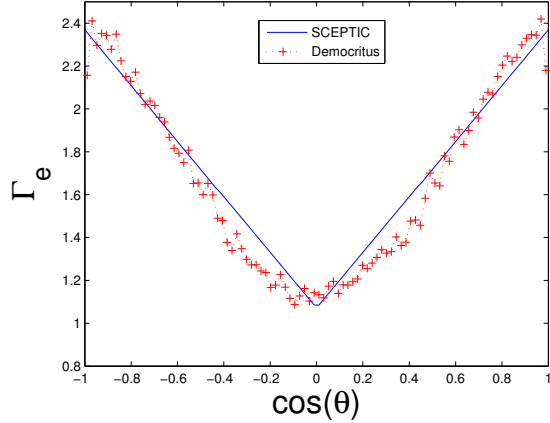
Table (1) compares the floating potentials as computed by *Democritus* and SCEPTIC. We notice that when SCEPTIC computes the electron flux using Eq. (16) and an accurate value for the shielding length such as the one given by Eq. (22) or a self-consistently calculated one, both codes agree to within 2%. This error can be explained by structural differences between the two codes such as the way the probe-plasma boundary is handled. Indeed because *Democritus* uses the immersed boundary technique, the probe potential is not unequivocally defined. Another relevant difference between the codes for the small domain we are using is the outer boundary geometry (spherical versus cylindrical).

	<i>Democritus</i>	SCEPTIC 1	SCEPTIC 2	SCEPTIC 3	SCEPTIC 4
S1	-1.47	-1.44	-1.45	-1.69	-1.17
S2	-1.59	-1.60	-1.61	-1.98	-1.41

Table 1: Comparison of the floating potentials (in units of  $T_e/e$ ) as computed by *Democritus* and SCEPTIC under different assumptions. SCEPTIC 1 : Electron flux given by Eq. (16) using a self-consistently calculated value of  $\lambda_s$  on each angular cell (Eq. (20)). SCEPTIC 2 : Electron flux given by Eq. (16) or Eq. (13) using a uniform  $\lambda_s$  given by Eq. (22). SCEPTIC 3 : Unmagnetized electron flux given by Eq. (4). SCEPTIC 4 : Strongly magnetized electron flux given by Eq. (5).

The validity of Eq. (16) can be further assessed by examining Fig. (10), where we compare the electron flux density ( $\Gamma_e$ ) to the sphere as given by both codes. The flux given by SCEPTIC is smooth since the only noise comes from the self-consistent evaluation of  $\lambda_s$  for each angular cell, and as a general rule in PIC codes noise on the potential is much lower than noise on particle position. The flux computed by *Democritus* has a slight drop at  $\cos\theta = \pm 1$  ; this non physical phenomenon can be explained by the fact that in order to keep the computation tractable we use too long a time-step to resolve the electron Larmor gyration accurately enough at the sphere edge. This however does not influence the total electron current, which in the case of a conducting sphere is the important value. A comparison of the total electron current to the sphere as calculated by both codes is given in Table (2), and the agreement is better than 3%.

a) Set 1



b) Set 2

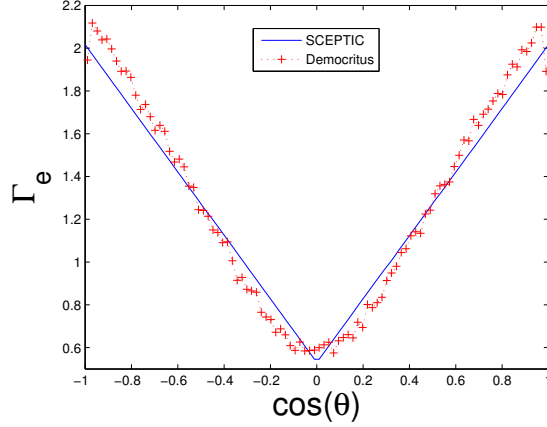


Figure 10: Electron flux density to the sphere as given by *Democritus* and SCEPTIC normalized to the ion thermal flux ( $v_{ti}/2\sqrt{\pi}$ ) for Set 1 ( $m_i/Zm_e = 100$ ,  $T_i = ZT_e$ ,  $\lambda_{De} = 2r_p$ ,  $v_d = 0$ ,  $\beta_e = 5.98$ ) and Set 2 ( $m_i/Zm_e = 100$ ,  $T_i = ZT_e$ ,  $\lambda_{De} = 2r_p$ ,  $v_d = 0.5\sqrt{T_e/Zm_i}$ ,  $\beta_e = 11.97$ ).

	<i>Democritus</i>	SCEPTIC 1	SCEPTIC 2	SCEPTIC 3	SCEPTIC 4
S1	1.68	1.73	1.73	1.85	1.58
S2	1.28	1.28	1.29	1.38	1.23

Table 2: Comparison of the total electron current ( $I_e$ ) normalized to the ion thermal current ( $4\pi r_p^2 v_{ti}/2\sqrt{\pi}$ ) as computed by *Democritus* and SCEPTIC under the same assumptions as in Table (1).

## 5 Floating potential dependence on a weak magnetic field in a stationary plasma

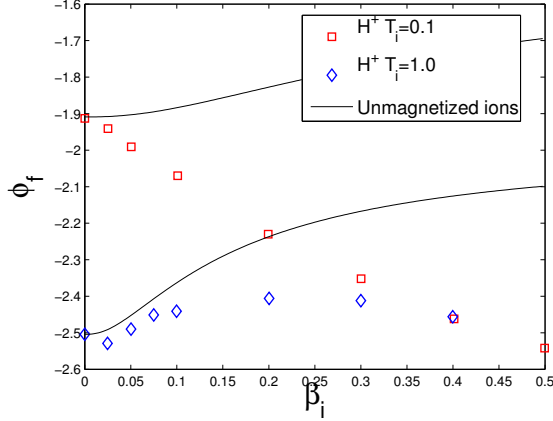
It has sometimes been argued that in the regime  $\beta_i \ll 1$  and  $\beta_e \gg 1$  one could calculate the probe floating potential  $\phi_f$  by assuming that the electrons are fully magnetized and the ions are unmagnetized (Tsytovich and al. [9]). This is equivalent to saying that the electron current is given by Eq. (5), and for a stationary conducting probe in the OML regime ( $\lambda_{De} \gg r_p$ ) the ion current is :

$$I_i^{OML} = 4\pi r_p^2 \frac{v_{ti}}{2\sqrt{\pi}} \left(1 - \frac{Z\phi_p T_e}{T_i}\right). \quad (24)$$

A more accurate expression for  $\phi_f$  is expected to be obtained by equating  $I_i^{OML}(\phi_f)$  (Eq. (24)) with  $I_e^*(\beta_e, \phi_f)$  (Eq. (13)).

As a concrete illustration of the new possibilities of SCEPTIC, we compared this analytical expression of  $\phi_f$  with self-consistent computations accounting for the ion magnetization,

a)  $v_d = 0, H^+$



b)  $v_d = 0, Ar^+$

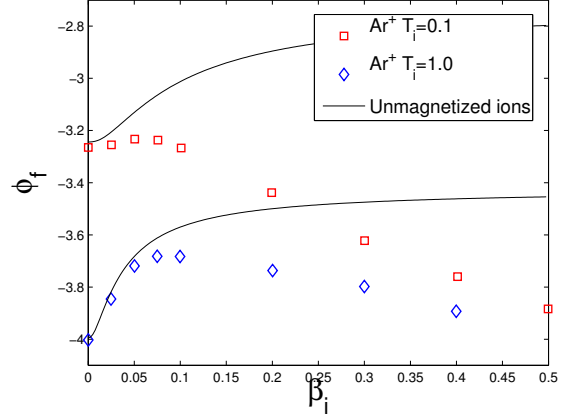


Figure 11: Floating potential  $\phi_f$  (In units of  $\frac{T_e}{e}$ ) as a function of  $\beta_i$  for Hydrogen and Argon ions,  $T_i = ZT_e$  and  $T_i = 0.1ZT_e$  (All the cases are run with  $\lambda_s = 2.3r_p$ ). The values of  $\phi_f$  given by  $I_i^{OML}(\phi_f) = I_e^*(\beta_e, \phi_f)$  are plotted as lines, while the self-consistent figures computed with SCEPTIC and accounting for both the electron and ion magnetization are plotted as squares and diamonds. The lines and points do not agree except at extremely small  $\beta_i$ .

as shown in Fig. (11). In order to accurately resolve the ion current dependence on small values of  $\beta_i$  we use a computational domain of radius  $r_b = 20r_p$ , but still assume  $\phi(r_b) = 0$ .

Clearly assuming unmagnetized ions is more appropriate for heavy hot ions, since  $\beta_e/\beta_i = \sqrt{m_i T_i / Z^2 m_e T_e}$ . However even for  $Ar^+$  at a fairly high temperature ( $T_i = T_e$ ) this approximation breaks down at a very small magnetic field. In the opposite regime ( $H^+$  at  $T_i = 0.1T_e$ ) the floating potential dependence on  $\beta_i$  is monotonically decreasing, meaning that the ion current drops faster than the electron current as the magnetic field rises. A regime such as the one suggested in [9] (unmagnetized ions, strongly magnetized electrons) therefore *never exists*, at least in a stationary plasma.

## 6 Summary

While the ion current collected by a negatively charged probe in the presence of background magnetic field depends on the whole potential distribution in the sheath and presheath, it has been shown that the shielding length  $\lambda_s$  (Eq. (20)) is the only space-charge figure relevant to the electron collection.

This allows one to find an empirical expression for the electron flux density to a spherical probe as a combination of the Upper and Lower bounds calculated by Rubinstein and Laframboise [2]. This flux is given by Eq. (17), and its evaluation only requires  $\lambda_s$ ,  $\beta_e$  (Magnetic field) and  $\phi_p$  (Probe potential distribution).

Since the shielding length is rarely known *a priori*, we also provide an empirical formula

for  $\lambda_s$  valid for the full range of plasma parameters (As long as the ions are only weakly magnetized). This formula is an improvement over past treatments and could also be used to calculate the probe capacitance at small Debye lengths.

Two applications of our treatment have been presented. It is first shown that it allows the hybrid PIC code SCEPTIC to run in the floating potential regime for an arbitrary magnetic field. This statement has been assessed by comparison with the full PIC code *Democritus*. Second, we compare the “real” evolution of the floating potential  $\phi_f$  with a rising magnetic field with the analytical value calculated by equating the OML current for the ions with the electron current given by Eq. (13). We find that even for heavy ions  $m_i/m_e$  is too small to have the electrons fully magnetized while the ions are still unmagnetized. This result could be modified in a flowing plasma.

## Acknowledgments

Leonardo Patacchini was supported in part by NSF/DOE Grant No. DE-FG02-06ER54891. The SCEPTIC calculations were performed on the Alcator Beowulf cluster which is supported by U.S. DOE Grant No. DE-FC02-99ER54512.

## References

- [1] I.H. Hutchinson *Principles of Plasma Diagnostics, Second edition* Cambridge University press (2002)
- [2] J. Rubinstein and J.G. Laframboise *Theory of a spherical probe in a collisionless magnetoplasma* Physics of Fluids **25**, 1174-1182 (1982)
- [3] L.J. Sonmor and J.G. Laframboise *Exact current to a spherical electrode in a collisionless, large Debye-length magnetoplasma* Physics of Fluids **3**, 2472-2490 (1991)
- [4] I.H. Hutchinson *Ion collection by a sphere in a flowing plasma: 2. non-zero Debye length* Plasma Phys. Control. Fusion **45**, 1477-1500 (2003)
- [5] G. Lapenta *Simulation of Charging and Shielding of Dust Particles in Drifting Plasmas* Physics of Plasmas **6** 1442-1447 (1999)
- [6] E.C. Whipple *PhD Thesis* George Washington University (1965)
- [7] J.E. Daugherty, R.K. Porteous, M.D. Kilgore and D.B. Graves *Sheath structure around particles in low-pressure discharges* J. Appl. Phys. **72**, 3934-3942 (1992)
- [8] I.H. Hutchinson *Collisionless ion drag force on a spherical grain* Plasma Phys. Control. Fusion **48**, 185-202 (2006)



- [9] V.N. Tsytovich, N. Sato and G.E. Morfill *Note on the charging and spinning of dust particles in complex plasmas in a strong magnetic field* New Journal of Physics **5**, 43.1-43.9 (2003)